Closing the Phenotypic Gap between Transformed Neuronal Cell Lines in Culture and Untransformed Neurons

Tereance A. Myers[1, 2], Cheryl A. Nickerson[3], Deepak Kaushal[1, 4], C. Mark Ott[5], Kerstin Höner zu Bentrup[4], Rajee Ramamurthy[6], Mayra Nelman-Gonzales[5], Duane L. Pierson[5], Mario T. Philipp[1, 4]

1 Division of Bacteriology & Parasitology, Tulane National Primate Research Center, 18703 Three Rivers Rd Covington, LA 70433, USA **2** Program in Molecular & Cellular Biology, School of Medicine, Tulane University Health Sciences Center, 1430 Tulane Ave. New Orleans, LA 70112, USA **3** Center for Infectious Diseases & Vaccinology, The Biodesign Institute, Arizona State University P.O. Box 875401 Tempe, AZ 85287, USA **4** Department of Microbiology & Immunology, School of Medicine, TUHSC, 1430 Tulane Ave. New Orleans, LA 70112, USA **5** Habitability and Environmental Factors Division, NASA-Johnson Space Center, Houston, TX 77058, USA **6** Department of Biological Sciences, Florida International University, University Park Campus, Miami, FL 33199

Correspondence: Mario T. Philipp, Division of Bacteriology and Parasitology, Tulane National Primate Research Center, Tulane University Health Sciences Center, 18703 Three Rivers Road, Covington, LA 70433, USA. Tel: 985 871 6221; fax: 985 871 6390; e-mail: philipp@tulane.edu

Abbreviations used: Bak, Bcl-2-antagonist/killer 1; Bax, Bcl-2-associated X protein; Bcl-2, B-cell lymphoma 2; BDNF, brain derived neurotrophic factor; CDK, cyclin dependent kinase; NRG1, neuregulin 1; CNS, central nervous system; HDAC, histone deacetylase; IPA, Ingenuity Pathways Analysis; ML, monolayer; N-myc, myelocytomatosis viral related oncogene; PI, propidium iodide; RA, retinoic acid; Rb, retinoblastoma; RWV, rotating wall vessel; SEM, scanning electron micrograph; ST, staurosporine; SY, SH-SY5Y; 3-D, three-dimensional; TG, thapsigargin

Total character count: 26, 081

Abstract

Studies of neuronal dysfunction in the central nervous system (CNS) are frequently limited by the failure of primary neurons to propagate *in vitro*. Neuronal cell lines can be substituted for primary cells but they often misrepresent normal conditions. We hypothesized that a 3-dimensional (3-D) cell culture system would drive the phenotype of transformed neurons closer to that of untransformed cells. In our studies comparing 3-D versus 2-dimensional (2-D) culture, neuronal SH-SY5Y (SY) cells underwent distinct morphological changes combined with a significant drop in their rate of cell division. Expression of the proto-oncogene N-myc and the RNA binding protein HuD was decreased in 3-D culture as compared to standard 2-D conditions. We observed a decline in the anti-apoptotic protein Bcl-2 in 3-D culture, coupled with increased expression of the pro-apoptotic proteins Bax and Bak. Moreover, thapsigargin (TG)-induced apoptosis was enhanced in the 3-D cells. Microarray analysis demonstrated significantly differing mRNA levels for over 700 genes in the cells of each culture type. These results indicate that a 3-D culture approach narrows the phenotypic gap between neuronal cell lines and primary neurons. The resulting cells may readily be used for *in vitro* research of neuronal pathogenesis.

Introduction

In vitro studies of disease pathogenesis in the CNS are often conducted with cultures of primary cells, but when the cells in question are neurons, in particular, human neurons, this becomes problematic. Because most post-embryonic neurons do not divide, their usefulness in primary culture is limited (1, 2). Transformed neuronal cell lines of both human and animal origin have thus become a requisite tool in studies of neuronal dysfunction in the CNS.

Although transformed neurons in cell lines will divide, they are known to exhibit an arrested state of cellular differentiation (3-7). Expression of the proto-oncogene N-myc is typically elevated and resistance to apoptosis is increased, making the interpretation of experimental results with these cells difficult when compared to their untransformed counterparts (6, 8-11).

Differentiation of transformed neurons in 2-D culture can be pursued by the addition of biochemical agents such as phorbol myristate acetate (PMA), retinoic acid (RA), staurosporine (ST) and brain-derived neurotrophic factor (BDNF) (12, 13) but it is not clear how closely these conditions model the cell-cell interactions that drive differentiation *in vivo*. Phorbol esters, for example, have been used to induce SY cells to differentiate toward a noradrenergic phenotype, while treatment with RA effects a cholinergic phenotype (13). Incubation of SY cells with either RA or PMA induces up-regulation of the anti-apoptotic proteins Bcl-2 and Bcl-x_L, whereas differentiation obtained with ST has been shown to notably diminish expression of these proteins (12, 14, 15). In each case, changes in resistance to apoptosis follow changes in expression of the markers. This is important because the Bcl-2 family proteins, including pro and anti-apoptotic members such as Bax, Bak and Bcl-2, figure prominently in molecular pathways of programmed cell death and may play a role in the degree of neuroblastoma cell tumorigenicity (16-19).

In addition to the limitations introduced by transformed cell lines, traditional monolayer or 2-D culture systems using flasks and multi-well dishes are often themselves inadequate to realistically model *in vivo* conditions (7, 20-22). Gravity induced sedimentation, non-homologous delivery of nutrients and a lack of cell-cell and cell-extra cellular matrix contacts are all potential limitations of 2-D cell culture (4, 5, 22, 23). Perhaps more importantly, 2-D cell culture approaches are also known to alter gene expression, to hinder cellular differentiation and the acquisition of polarity, and to prevent formation of the complex 3-D cellular architecture commonly found in an intact tissue (5, 7, 22, 24-27). While matrigel, collagen, peptide and synthetic nanofiber scaffolds are each being used and developed as more realistic procedures for *in vitro* cell culture (5, 7, 21, 25), NASA engineered rotating wall vessels (RWV) are also being employed to establish a fluid suspension culture that is capable of inducing biologically meaningful 3-D growth *in vitro* (4, 23, 28, 29). During culture in a RWV, individual cells aggregate into 3-D tissue-like assemblies developing enhanced states of differentiation and cross communication through cell-cell contacts. Gas exchange and nutrient delivery are optimized under these conditions, (4, 22) and the cellular phenotypes, as compared to their 2-D cultured counterparts, become functionally and morphologically similar to the parental tissues and organs that they represent (7, 20, 29-32).

Our lab is interested in studying the pathogenesis of Lyme neuroborreliosis. This disease is caused by infection with the spirochete *Borrelia burgdorferi.* We and others have argued that the associated neurocognitive symptoms of this disease are precipitated by neuronal dysfunction resulting from inflammatory effects elicited by the spirochete (33-35). The inherent limitations of primary neuronal culture *in vitro* prompted us to incorporate transformed neurons into our research design. As molecular and cellular changes that accompany the conversion of normal

cells into states of disease or malignancy are altered by 2-D growth (4, 28, 36), we wanted to establish a 3-D model of *in vitro* neuronal culture, to assess whether this procedure would attenuate the phenotypic differences that exist between transformed and untransformed neurons.

The SY cell line is an adrenergic "n" type clone of the "mixed cell" human neuroblastoma line SK-N-SH and has been used extensively in standard 2-D cultures to study neuronal function, growth, damage in response to insult, degeneration and differentiation (3, 13, 14, 37-39). By culturing SY cells under gentle, low-shear conditions in a RWV, we have succeeded in obtaining a cell line that expresses classic morphological and functional patterns of neuronal differentiation. We believe that the enhanced state of differentiation and cell-cell crosstalk events generated by culture in 3-D, bypasses the need for chemical treatment of the cells, and provides a more normalized cellular response during experimental studies.

Results

3-D culture changes the morphology and proliferation rate in SY neuronal cells

SY cells cultured for 21 d in the RWV, and then for counting purposes, transferred back to 2-D culture flasks for 5 d, revealed a decrease in the cell doubling rate from 40 h to approximately 65 h, with no change in cell viability (Fig.1 A). Because the carrier beads used in our 3-D culture were coated in collagen, we additionally cultured SY cells for 3 and for 4 wks in 2-D flasks coated with collagen. We observed no detectable difference in the morphology, cell viability or doubling rate of 2-D cells cultured on plastic as compared to collagen. Scanning electron microscopy (SEM) revealed important differences in the morphology of SY cells cultured in 2-D or in 3-D. Specifically, only the 3-D-cultured SY cells acquired a parental, tissue-like conformation with dramatic increases in neurite extension, direction and number (Fig. 1 B).

Decreased expression of N-myc and HuD

Human neuroblastoma cells are typically characterized by de-differentiation. They have re-entered S-phase of the cell cycle, and are highly resistant to apoptosis (9, 11). Amplified expression of the proto-oncogene N-myc has been correlated with cellular de-differentiation and increased resistance to apoptosis, and is believed to have a crucial role in maintenance of the cells' malignant phenotype (6, 10, 40, 41). The RNA binding protein HuD functions in stabilizing N-myc mRNA and may consequently enhance steady-state expression levels of this oncogene (40-42). Reduced expression of the HuD protein could therefore contribute, through destabilization of N-myc, to an increase in cellular differentiation.

Western analysis confirmed a culture-dependent shift in protein expression of these markers, with the decrease positively correlating to the length of time the cells had spent in 3-D culture

(Fig. 2 A). Images obtained with confocal microscopy revealed a diminished level of N-myc and HuD protein expression in SY cells cultured in 3-D as opposed to 2-D (Fig. 2 B).

Apoptosis resistance is diminished in 3-D cultured SY and PC12 cells

Cells over-expressing the anti-apoptotic protein Bcl-2 or cells with depleted pro-apoptotic Bax and Bak exhibit resistance to cell death as induced by mitochondrial dysfunction and ER stress (18, 19, 43, 44). Because increased resistance to apoptosis is one hallmark of a transformed phenotype in many cancer cell lines, we were interested in exploring the effects of 3-D culture on the expression of key proteins in the apoptosis pathway. We found a decreased expression of Bcl-2 coupled with increased Bax and Bak proteins in 3-D cultured SY cells as compared to those cultured in standard 2-D conditions (Fig. 3 A). While confocal imaging clearly indicated increased Bak protein in 3-D cultured cells, western analysis was not sensitive enough to detect its expression.

Our next consideration was to assess apoptosis functionally and to confirm that our findings were not restricted to a single cell line. PC12 is a rat pheochromocytoma cell line that can be stimulated with nerve growth factor to differentiate into sympathetic-like neurons (45) Due to their induced ability to cease division, become electrically excitable and extend neurites, PC12 cells have become an extremely well characterized *in vitro* model for studies of neuronal differentiation and survival (20, 46-49).

TG is known to induce apoptosis through the passive release of Ca^{2+} from ER stores. These events lead to subsequent increases in cytosolic Ca^{2+}, stressing both the ER and the mitochondria (16-19, 50). In order to determine inherent differences in apoptosis between the 3-D and 2-D cultured cells we used the TUNEL assay. SY cells were incubated with 10 nM TG for 24 hours

and for 5 days. The 3-D-cultured SY cells were treated either inside of the RWV, 3-D(RWV) or after transfer back into standard culture flasks (3-D). We additionally incubated PC12 cells with 30 nM TG, for 5 d. All of the 3-D-cultured PC12 cells were treated after transfer back into standard culture flasks. The SY and PC12 cells grown in 2-D culture were treated in their respective dishes.

In a 5 d comparison of TG-stimulated versus non-stimulated control cells, we found an approximate 4-7 fold increase in the occurrence of apoptosis in 3-D as opposed to 2-D culture. In a similar 5 d comparison, 3-D cultured PC12 cells were approximately 3-fold more susceptible to apoptosis than were the 2-D cells. At 24 h, a noticeable difference in the degree of apoptosis occurring in stimulated versus control cells was found only in the 3-D(RWV) cells (Fig. 3 B).

SY cells maintain 3-D culture-induced alterations in the phenotypic markers N-Myc and Bcl-2 for at least 5 d after return to 2-D culture

As many studies of neuronal pathogenesis involve co-cultures of neuronal cell lines with primary glia and/or other live organisms propagated in 2-D culture, we wanted to evaluate the length of time that SY cells would retain a 3-D phenotype once they were transferred back into 2-D culture. We thus examined the expression of N-myc and Bcl-2, two molecular markers closely related to both differentiation and tumorigenicity (6, 8-11, 14, 15, 19). Assessment of the SY cells that had been "pre-conditioned" in 3-D culture for approximately 3 wks and were then removed to 2-D culture revealed a five-day experimental window during which reversion of the culture-induced changes were minimal (Fig. 4).

Microarray analysis of gene expression in SY cells cultured in 3-D and in 2-D

In an effort to expand and to further clarify our findings related to the states of differentiation and morphology in 2-D and 3-D-cultivated SY cells, we employed microarray analysis to observe the culture-induced effects on global gene expression. Because abnormalities in the expression and activity of multiple genes often work in concert to affect a transformed cellular phenotype, (51-54) Ingenuity Pathways Analysis (IPA) software was used to compare the mRNA levels in 44,544 70-mer oligos corresponding to over 24,000 human genes. Cancer, cell morphology and proliferation pathways were among those found to be the most altered (Fig. 5 A). The G1/S and G2/M cell cycle check points, as well as the p53 and neuregulin signaling pathways were also significantly affected (Fig. 5 B).

Along with abnormalities in the p53 tumor suppressor gene pathway, dysregulation of the cell cycle is one of the most frequent alterations found in tumor development, with the inappropriate progression of G1/S being especially common (52, 53, 55, 56) In the normal dividing cell, cyclin-dependent kinases (CDKs) form a complex with D/E-type cyclins to phosphorylate the retinoblastoma (Rb) gene, causing the release of bound E2F family transcription factors. These now unbound E2F proteins then act to drive G1/S phase transition by the activation (or repression) of multiple gene targets affecting cellular growth and proliferation, nucleotide metabolism and DNA synthesis (53, 54, 57-59). Histone deacetylases (HDAC's) form a complex with bound E2F proteins and are also released upon phosphorylation of Rb. Importantly, HDAC inhibitors have been shown to cause cell cycle arrest in G1 and to function in cellular differentiation and apoptosis (60, 61). Because of its strong ties to transformation, we wanted to look more closely at the actual variance reported in the G1/S pathway.

The CDK4/6 inhibitor CDKN2B was found to be significantly up-regulated in 3-D versus 2-D cultured SY cells. At the same time, the transcription factor E2F3, HDAC2 and the neuregulin1

(NRG1) gene, whose product promotes growth and proliferation in neuronal cells of the peripheral and central nervous systems (62, 63), were each significantly down regulated (Fig. 5 C, Table 1). These events clearly indicate arrest in G1. Rb gene expression was also decreased, but without knowing the phosphorylation state of this gene, correlation to the cell cycle is questionable.

RT-PCR confirms the differential expression of G1/S cell-cycle check point genes in 3-D versus 2-D cultured SY cells

A significant part of our microarray analysis was focused on exploring culture-induced differential gene expression in a neuronal cell line that could indicate phenotypic reversion toward a more normalized state. Pathways such as growth and proliferation or the cell cycle checkpoints were of interest. We used RT-PCR to confirm our initial array findings. In order to maintain integrity in this experiment as compared to our microarray analysis, we used aliquots of the same SY 3D and 2-D cell RNA that was collected for each of the arrays. Expression changes in 3 of the 4 selected genes known to influence the G1/S cell cycle checkpoint matched our microarray data (Fig. 5 C2, Table 2).

Discussion

It is generally accepted that once developing neurons leave the ventricular and sub-ventricular zones of the CNS, they are terminally differentiated and become persistently postmitotic (56, 64, 65). Although some neurons are generated in the adult brain, neuronal exit from the cell cycle is typically viewed as permanent (56, 64-67). This inability to divide often complicates research requiring primary neuronal cultures. While a handful of human neuronal cell lines are available

to researchers, the transformed phenotype of these cells is less than optimal. In consideration of these circumstances, we have applied a transitional cell culture technique to neuronal cell lines that attenuates some of the aberrant features characteristic of transformed neurons.

Loss of cellular differentiation combined with an unchecked potential to proliferate has long been a hallmark in the progression of tumorigenesis (53, 54, 64, 67). In this report we have shown that the morphology and proliferation characteristics of 3-D-cultivated SY cells align more with a parental untransformed phenotype than those grown in 2-D. The two classic prognostic markers of tumorigenicity in neuroblastoma, N-myc and HuD expression, are diminished in 3-D as compared to 2-D-cultured SY cells. A decline in the amount of HuD mRNA and protein in various cell lines has been shown to cause a marked reduction in steady-state levels of mature N-myc mRNA and protei, (6, 10, 11, 40-42) thus even small decreases in HuD protein may be contributing, via the effect on N-myc, to increased cellular differentiation in 3-D cultured SY cells.

Numerous reports verify the ability of 3-D growth to sway cellular characteristics toward those of a less transformed state as compared with that of 2-D culture (5, 7, 14, 20, 22, 23, 26, 36, 68, 69). In 1997, Bissell et al showed that breast cancer cells grown in 3-D culture changed their transformed behavior to that of non-cancerous cells, resuming a normalized morphology combined with more typical patterns of growth and proliferation (5, 25). Nickerson et al. further demonstrated that culture in 3-D can promote cellular differentiation and polarity, some of the key elements perturbed in transformation (22, 23, 26, 68, 69). While researchers have followed different protocols for 3-D culture, e.g. growth on gels and matrices versus fluid culture in a RWV, the trend toward a less transformed phenotype is preserved in numerous cell types. In our model, SY cells “normalized” in 3-D culture, were able to maintain a less transformed phenotype

for at least 5 d after return to 2-D growth conditions. Given that cell cultures in a 2-D format are generally easier to handle during experimental procedures, than are cells in 3-D culture, this finding adds to the practicality of our model.

Further distancing transformed cells from the normal tissues that they are intended to represent is an increased resistance to apoptosis (36, 49, 53). We have found 3-D-cultured SY and PC12 cells to be more susceptible to TG-induced apoptosis than the same cells grown in 2-D. Because of TG's known association to the intrinsic pathway of ER and mitochondrial induced mortality in which Bcl-2 family proteins are highly implicated, changes in the anti-apoptotic protein Bcl-2 and pro-apoptotic family members Bax and Bak, provided a possible mechanism contributing to the enhanced apoptotic response (17-19). Interestingly, while stimulation with ST diminishes the expression of Bcl-2 in 2-D-cultivated SY cells, chemical differentiation with RA or the phorbol ester TPA has been shown to up-regulate Bcl-2 expression in these cells (3, 13, 14, 70, 71). While the latter situation could be viewed as a more "protected" condition for the differentiated and thus (now) postmitotic neurons, resistance to signals of apoptosis above that of a cancerous state seems incongruous with a less transformed phenotype.

The primary hypothesis addressed in this study was that a 3-D culture system would drive the phenotype of transformed neurons closer to that of untransformed cells. We have noted culture induced changes in the morphology and biomarker expression of our 3-D cultured SY cells, reflecting a more differentiated, and thus a less transformed phenotype. We have shown apoptosis resistance to be diminished and have observed a decline in the 3-D cultured SY cell doubling rate. Microarray analysis comparing 3-D and 2-D-cultivated SY cells provided a strong indication that alterations in the G1/S cell cycle progression were contributing to the diminished doubling rate in the 3-D cultured SY cells. Neuronal cells arrested at this checkpoint are known

to either return to G0 and re-differentiate, or they will die by apoptosis (67). Due to the decline in doubling rate and the near 100 percent viability of our 3-D cultured SY cells, we believe that a return to quiescence is occurring. Confirmation of the array results involved in this pathway was obtained using QRT-PCR. Lending added support to our hypothesis, culture-induced variance in several other prominent pathways leading to transformation and cancer, were also identified on the array.

The use of microarray analysis to screen for the differential expression of SY cell genes propagated in 2-D and 3-D culture conditions has been employed by other investigators (39, 72). While focusing on differences in morphology and neurite outgrowth, Li et al, found more than 1700 of 14,564 genes to be differentially regulated in SY cells propagated on collagen matrices. Based on the number of genes being modified, it is reasonable that phenotypic changes beyond those of morphology and neurite extension are occurring. These results, like our own, indicate that continued research in this area will be needed to fully characterize the culture induced changes in gene expression that define 3-D versus 2-D-cultured cells.

The generation of purified primary neurons in numbers satisfactory for experimental study is difficult to achieve with animal cells, and is nearly impossible with human cells. Researchers must therefore rely on transformed cell lines for many studies of pathogenesis in the CNS. The ability to provide a more normalized cellular environment *in vitro* has improved dramatically over the past decades, particularly with the use of 3-D culture systems (4, 5, 7, 22, 23, 26, 73, 74). The application of this technique to human neuronal culture is particularly attractive in view of the cells' post-mitotic constraints in primary culture. We have shown here that 3-D culture evokes changes in SY cell morphology, proliferation, apoptosis resistance and differentiation states in a manner that narrows the phenotypic gap between those cells and their non-transformed

counterparts. As studies involving human neuronal pathogenesis remain largely dependent on *in vitro* cell culture, this approach may easily be further exploited to create a more realistic environment in which to model nerve cell function and response.

Material and Methods

Cell Culture and Reagents

2-D System

Human SY neuroblastoma cells (American Type Tissue Culture Collection ATCC CRL-2266) and PC12 rat pheochromocytoma cells (ATCC CRL-1721) were each seeded into separate T75 flasks with medium renewal every 3-7 d. The culture flasks for PC12 cells were coated with PureCol collagen (Inamed). Cell propagation was performed as per the ATCC product sheet. Nerve Growth Factor (Sigma) was added to the PC12 medium at 50 ng/2-D. Penicillin (100 units/ml), streptomycin (100 units/ml) and amphotericin B (0.25 μg/ml) (Gibco/Invitrogen) were added to all media. Trypsin(2.5%)/EDTA(0.38 g/L) was used to dislodge the cells, and Trypan Blue stain was used in assessing cell viability, (Gibco/Invitrogen). 2-D samples were harvested at a passage ≤ 20.

3-D System

Approximately 10^7 viable 2-D-cultured SY or PC12 cells were dislodged by trypsin and loaded into 50 ml RWVs (Synthecon) containing 200 mg of Cytodex-3 micro-carrier beads (Amersham Biosciences) suspended in complete growth medium (ATCC product sheet). Entirely filled vessels were then attached to a rotator base (Synthecon) with initial speeds typically set at 18-22 RPM. The RPM were adjusted during cultivation to maintain the cell aggregates in suspension. Complete removal of all bubbles was addressed upon initial rotation and daily thereafter. Cell viability assays and medium replacement were performed every 2-5 d. 3-D cells were collected after 2-4 wk (see individual results) of culture. Although minimal changes were noted at 2 wk, we typically found significant molecular marker differences at the 3 wk time points with small additional changes at 4 wk. For efficiency, 3 wk was used as our standard.

Cell Counting and Proliferation Assays

3-D cultures were removed from the RWV, dislodged from the cytodex beads by treatment with trypsin/EDTA, and then dissociated from the beads with 40 μm cell strainers (Becton Dickenson). 10^6 2-D and 3-D cultured SY cells were independently seeded into 10 ml of complete growth medium in T75 culture dishes and allowed to propagate for 5 d. Cells were them removed from the dish, (trypsin/EDTA), and counted in a BrightLine Hemocytometer.

Morphology: Light and Electron Microscopy

Live cell photographs were imaged with a Sony Cyber Shot digital still camera (DSCF717) attached to a Nikon TMS light microscope. SEM was used to examine changes in the morphology of SY cells as described previously with minor modifications (22). 2-D cells and 3-D cell aggregates were fixed in 3% glutaraldehyde, 0.5% paraformaldehyde, in PBS pH 7.2 for a minimum of 24 h. The samples were flushed in triplicate with filter-sterilized deionized water to remove salts and then transferred for observation to a Philips XL 30 ESEM (FEI Co.) Chamber pressure was adjusted between 1 and 2 torr to optimize image quality.

Confocal Microscopy

2-D and 3-D cells removed from culture were washed once in PBS and fixed in 2% paraformaldehyde (PFA) (USB Corporation) for 5-10 min, permeablized in PBS with fish skin gelatin (Sigma-Aldrich) and Triton X-100 (ICN Biomedicals) (PBS/FSG/Triton) and blocked in 10% normal goat serum (Gibco). The fixed 2-D and 3-D cultured cells were equally stained with

primary antibodies for 1 h, washed 3 times in PBS and then stained with corresponding secondary antibodies for 45 min. Nuclear stains were combined with the secondary antibodies at a concentration of 0.05 μg/ml. Primary antibodies used include anti-N-myc, HuD, Bcl-2, Bax and Bak, (Santa Cruz Biotechnology). Alexa-488 (green)-conjugated secondary antibodies, and the To-Pro (blue) nuclear stains were from Invitrogen. Propidium Iodide (PI) (red) (Sigma-Aldrich) was used as an alternative nuclear stain. Imaging was performed using a Leica TCS SP2 confocal microscope equipped with three lasers (Leica Microsystems). Six to eighteen 0.2 μm optical slices per image were collected at 512 x 512 pixel resolution. The pinhole size, gain and contrast, filter settings, and laser output were held constant for each comparison of the 2-D and 3-D image sets.

Western Blot Analysis

Cells were lysed on ice for 10 min using buffer (0.15 M NaCl, 5 mM EDTA, pH 8, 1% Triton X-100, 10 mM Tris-HCl, pH 7.4) containing 5 mM DTT and a Protease Inhibitor Cocktail for mammalian cells (Sigma-Aldrich). Protein concentrations were measured with the BCA assay (Pierce Biotechnology). After optimization for each sample, total protein (40 μg/lane for N-myc, HuD, Bcl-2, and Bak, and 50 μg/lane for Bax) was resolved in 12% Tris-Hcl pre-cast gels (BioRad), and electrophoretically transferred to nitrocellulose Protran membranes (Schleicher and Schuell BioSciences). Non-specific binding was blocked with 3% BSA fraction V (Sigma-Aldrich) in PBS-tween (PBST) at 4°C over night. Target proteins were detected with rabbit or mouse primary antibodies for 2 h at room temperature or at 4°C over night (all antibodies were from Santa Cruz Biotech. except for β-actin (Abcam). The blots were washed 3 times in PBST and incubated for 45 min with horseradish peroxidase-conjugated anti-rabbit or anti-mouse

secondary antibodies (Santa Cruz Biotech.) The blots were again washed 3 times in PBST, developed for 1-2 min in Western Blot Luminol Reagent (SCB) and visualized using a Kodak Imager 2000 and Kodak Image Analysis Software.

Apoptosis assays

SY cells (1 x 10^6) cultured in 2-D or in 3-D were incubated with or without 10 nM TG. The 2-D and 3-D cells were harvested using trypsin, washed in PBS, and fixed for 5-10 min in 2% PFA. Prior to fixation, the 3-D-cultured cells treated inside of the RWV were separated from the beads using a 40 μm cell strainer (Becton Dickinson). The fixed cells were permeablized in PBS/FSG/Triton and blocked with 10% NGS. Apoptosis was evaluated using the Apoptag TUNEL assay kit (Chemicon). The results were analyzed using a Leica TCS SP2 confocal microscope as described above. Cell morphology consistent with apoptosis including cell shrinkage, nuclear condensation and membrane blebbing were assessed along with the fluorescein staining for TUNEL. The number of apoptotic cells counted was divided by the total (500 minimum) number of cells counted. This protocol was also followed for evaluation of apoptosis in PC12 cells. Due to an increased drug tolerance, 30 nM TG was used in the PC12 assay. 3-D-cultured PC12 samples were stimulated for 5 d after removal from the RWV to multi-well dishes.

Microarray

Microarray experiments and analysis of data was performed according to previously described protocols (75, 76). Further details are available in the Supplemental data section.

QRT-PCR

RNA was collected as for the microarray analysis. The QuantiFast SYBR Green RT-PCR kit (Qiagen) was used for the QRT-PCR. All assays were performed as per manufacturer's instruction with Qiagen QuantiTect primer pairs in a 96-well block ABI 7700 RT cycler.

References:

1. Smith, C.U.M. 1996. Elements of Molecular Neurobiology John Wiley and Sons, Ltd, Chichester. 522 pp.
2. Encinas, M., M. Iglesias, Y. Liu, H. Wang, A. Muhaisen, V. Cena, C. Gallego, and J.X. Comella. 2000. Sequential treatment of SH-SY5Y cells with retinoic acid and brain-derived neurotrophic factor gives rise to fully differentiated, neurotrophic factor-dependent, human neuron-like cells. *Journal of neurochemistry* 75:991-1003.
3. Hanada, M., S. Krajewski, S. Tanaka, D. Cazals-Hatem, B.A. Spengler, R.A. Ross, J.L. Biedler, and J.C. Reed. 1993. Regulation of Bcl-2 oncoprotein levels with differentiation of human neuroblastoma cells. *Cancer research* 53:4978-4986.
4. Guidi, A., G. Dubini, F. Tominetti, and M. Raimondi. 2002. Mechanobiologic Research in a Microgravity Environment Bioreactor. 1-9.
5. Abbott, A. 2003. Cell culture: biology's new dimension. *Nature* 424:870-872.
6. van Golen, C.M., M.E. Soules, A.R. Grauman, and E.L. Feldman. 2003. N-Myc overexpression leads to decreased beta1 integrin expression and increased apoptosis in human neuroblastoma cells. *Oncogene* 22:2664-2673.
7. Zhang, S. 2004. Beyond the Petri dish. *Nature biotechnology* 22:151-152.
8. Fan, L., J. Iyer, S. Zhu, K.K. Frick, R.K. Wada, A.E. Eskenazi, P.E. Berg, N. Ikegaki, R.H. Kennett, and C.N. Frantz. 2001. Inhibition of N-myc expression and induction of apoptosis by iron chelation in human neuroblastoma cells. *Cancer research* 61:1073-1079.
9. van Noesel, M.M., R. Pieters, P.A. Voute, and R. Versteeg. 2003. The N-myc paradox: N-myc overexpression in neuroblastomas is associated with sensitivity as well as resistance to apoptosis. *Cancer letters* 197:165-172.
10. Smith, A.G., N. Popov, M. Imreh, H. Axelson, and M. Henriksson. 2004. Expression and DNA-binding activity of MYCN/Max and Mnt/Max during induced differentiation of human neuroblastoma cells. *Journal of cellular biochemistry* 92:1282-1295.
11. Kang, J.H., P.G. Rychahou, T.A. Ishola, J. Qiao, B.M. Evers, and D.H. Chung. 2006. MYCN silencing induces differentiation and apoptosis in human neuroblastoma cells. *Biochemical and biophysical research communications* 351:192-197.
12. Lombet, A., V. Zujovic, M. Kandouz, C. Billardon, S. Carvajal-Gonzalez, A. Gompel, and W. Rostene. 2001. Resistance to induced apoptosis in the human neuroblastoma cell line SK-N-SH in relation to neuronal differentiation. Role of Bcl-2 protein family. *European journal of biochemistry / FEBS* 268:1352-1362.
13. Garcia-Gil, M., R. Pesi, S. Perna, S. Allegrini, M. Giannecchini, M. Camici, and M.G. Tozzi. 2003. 5'-aminoimidazole-4-carboxamide riboside induces apoptosis in human neuroblastoma cells. *Neuroscience* 117:811-820.
14. Ribas, J., and J. Boix. 2004. Cell differentiation, caspase inhibition, and macromolecular synthesis blockage, but not BCL-2 or BCL-XL proteins, protect SH-SY5Y cells from apoptosis triggered by two CDK inhibitory drugs. *Experimental cell research* 295:9-24.
15. Pregi, N., D. Vittori, G. Perez, C.P. Leiros, and A. Nesse. 2006. Effect of erythropoietin on staurosporine-induced apoptosis and differentiation of SH-SY5Y neuroblastoma cells. *Biochimica et biophysica acta* 1763:238-246.

16. Nechushtan, A., C.L. Smith, I. Lamensdorf, S.H. Yoon, and R.J. Youle. 2001. Bax and Bak coalesce into novel mitochondria-associated clusters during apoptosis. *The Journal of cell biology* 153:1265-1276.
17. Zong, W.X., C. Li, G. Hatzivassiliou, T. Lindsten, Q.C. Yu, J. Yuan, and C.B. Thompson. 2003. Bax and Bak can localize to the endoplasmic reticulum to initiate apoptosis. *The Journal of cell biology* 162:59-69.
18. Scorrano, L., S.A. Oakes, J.T. Opferman, E.H. Cheng, M.D. Sorcinelli, T. Pozzan, and S.J. Korsmeyer. 2003. BAX and BAK regulation of endoplasmic reticulum Ca2+: a control point for apoptosis. *Science (New York, N.Y* 300:135-139.
19. Elyaman, W., F. Terro, K.C. Suen, C. Yardin, R.C. Chang, and J. Hugon. 2002. BAD and Bcl-2 regulation are early events linking neuronal endoplasmic reticulum stress to mitochondria-mediated apoptosis. *Brain research* 109:233-238.
20. Lelkes, P.I., D.L. Galvan, G.T. Hayman, T.J. Goodwin, D.Y. Chatman, S. Cherian, R.M. Garcia, and B.R. Unsworth. 1998. Simulated microgravity conditions enhance differentiation of cultured PC12 cells towards the neuroendocrine phenotype. *In vitro cellular & developmental biology* 34:316-325.
21. O'Brien, L.E., M.M. Zegers, and K.E. Mostov. 2002. Opinion: Building epithelial architecture: insights from three-dimensional culture models. *Nature reviews* 3:531-537.
22. Nickerson, C.A., T.J. Goodwin, J. Terlonge, C.M. Ott, K.L. Buchanan, W.C. Uicker, K. Emami, C.L. LeBlanc, R. Ramamurthy, M.S. Clarke, C.R. Vanderburg, T. Hammond, and D.L. Pierson. 2001. Three-dimensional tissue assemblies: novel models for the study of Salmonella enterica serovar Typhimurium pathogenesis. *Infection and immunity* 69:7106-7120.
23. LaMarca, H.L., C.M. Ott, K. Honer Zu Bentrup, C.L. Leblanc, D.L. Pierson, A.B. Nelson, A.B. Scandurro, G.S. Whitley, C.A. Nickerson, and C.A. Morris. 2005. Three-dimensional growth of extravillous cytotrophoblasts promotes differentiation and invasion. *Placenta* 26:709-720.
24. Freshney, R.I. 2000. Culture of Animal Cells; A Manual of Basic Technique. Wiley-Liss, Inc., New York.
25. Schmeichel, K.L., and M.J. Bissell. 2003. Modeling tissue-specific signaling and organ function in three dimensions. *Journal of cell science* 116:2377-2388.
26. Honer zu Bentrup, K., R. Ramamurthy, C.M. Ott, K. Emami, M. Nelman-Gonzalez, J.W. Wilson, E.G. Richter, T.J. Goodwin, J.S. Alexander, D.L. Pierson, N. Pellis, K.L. Buchanan, and C.A. Nickerson. 2006. Three-dimensional organotypic models of human colonic epithelium to study the early stages of enteric salmonellosis. *Microbes and infection / Institut Pasteur* 8:1813-1825.
27. Eisenstein, M. 2006. Thinking Outside the Dish. *Nature Methods* 3:1035-1043.
28. Gao, H., P.S. Ayyaswamy, and P. Ducheyne. 1997. Dynamics of a microcarrier particle in the simulated microgravity environment of a rotating-wall vessel. *Microgravity science and technology* 10:154-165.
29. Nickerson, C.A., and C.M. Ott. 2004. A New Dimension in Modeling Infectious Disease. In ASM News. 169-175.
30. Hammond, T.G., and J.M. Hammond. 2001. Optimized suspension culture: the rotating-wall vessel. *American journal of physiology* 281:F12-25.
31. Unsworth, B.R., and P.I. Lelkes. 1998. Growing tissues in microgravity. *Nature medicine* 4:901-907.

32. Nickerson, C.A., E.G. Richter, and C.M. Ott. 2007. Studying host-pathogen interactions in 3-D: organotypic models for infectious disease and drug development. *J Neuroimmune Pharmacol* 2:26-31.
33. Ramesh, G., A.L. Alvarez, E.D. Roberts, V.A. Dennis, B.L. Lasater, X. Alvarez, and M.T. Philipp. 2003. Pathogenesis of Lyme neuroborreliosis: Borrelia burgdorferi lipoproteins induce both proliferation and apoptosis in rhesus monkey astrocytes. *European journal of immunology* 33:2539-2550.
34. Livengood, J.A., and R.D. Gilmore, Jr. 2006. Invasion of human neuronal and glial cells by an infectious strain of Borrelia burgdorferi. *Microbes and infection / Institut Pasteur* 8:2832-2840.
35. Rasley, A., S.L. Tranguch, D.M. Rati, and I. Marriott. 2006. Murine glia express the immunosuppressive cytokine, interleukin-10, following exposure to Borrelia burgdorferi or Neisseria meningitidis. *Glia* 53:583-592.
36. Kunz-Schughart, L.A., K. Groebe, and W. Mueller-Klieser. 1996. Three-dimensional cell culture induces novel proliferative and metabolic alterations associated with oncogenic transformation. *International journal of cancer* 66:578-586.
37. Biedler, J.L., L. Helson, and B.A. Spengler. 1973. Morphology and growth, tumorigenicity, and cytogenetics of human neuroblastoma cells in continuous culture. *Cancer research* 33:2643-2652.
38. Ho, R., J.E. Minturn, T. Hishiki, H. Zhao, Q. Wang, A. Cnaan, J. Maris, A.E. Evans, and G.M. Brodeur. 2005. Proliferation of human neuroblastomas mediated by the epidermal growth factor receptor. *Cancer research* 65:9868-9875.
39. Martinez, T., and A. Pascual. 2007. Identification of genes differentially expressed in SH-SY5Y neuroblastoma cells exposed to the prion peptide 106-126. *The European journal of neuroscience* 26:51-59.
40. Chagnovich, D., and S.L. Cohn. 1996. Binding of a 40-kDa protein to the N-myc 3'-untranslated region correlates with enhanced N-myc expression in human neuroblastoma. *The Journal of biological chemistry* 271:33580-33586.
41. Grandinetti, K.B., B.A. Spengler, J.L. Biedler, and R.A. Ross. 2006. Loss of one HuD allele on chromosome #1p selects for amplification of the N-myc proto-oncogene in human neuroblastoma cells. *Oncogene* 25:706-712.
42. Lazarova, D.L., B.A. Spengler, J.L. Biedler, and R.A. Ross. 1999. HuD, a neuronal-specific RNA-binding protein, is a putative regulator of N-myc pre-mRNA processing/stability in malignant human neuroblasts. *Oncogene* 18:2703-2710.
43. Henshall, D.C., T. Araki, C.K. Schindler, J.Q. Lan, K.L. Tiekoter, W. Taki, and R.P. Simon. 2002. Activation of Bcl-2-associated death protein and counter-response of Akt within cell populations during seizure-induced neuronal death. *J Neurosci* 22:8458-8465.
44. Murakami, Y., E. Aizu-Yokota, Y. Sonoda, S. Ohta, and T. Kasahara. 2007. Suppression of endoplasmic reticulum stress-induced caspase activation and cell death by the overexpression of Bcl-xL or Bcl-2. *Journal of biochemistry* 141:401-410.
45. Greene, L.A., and A.S. Tischler. 1976. Establishment of a noradrenergic clonal line of rat adrenal pheochromocytoma cells which respond to nerve growth factor. *Proceedings of the National Academy of Sciences of the United States of America* 73:2424-2428.
46. Das, P.C., W.K. McElroy, and R.L. Cooper. 2000. Differential modulation of catecholamines by chlorotriazine herbicides in pheochromocytoma (PC12) cells in vitro. *Toxicol Sci* 56:324-331.

47. Attiah, D.G., R.A. Kopher, and T.A. Desai. 2003. Characterization of PC12 cell proliferation and differentiation-stimulated by ECM adhesion proteins and neurotrophic factors. *Journal of materials science* 14:1005-1009.
48. Vyas, S., P. Juin, D. Hancock, Y. Suzuki, R. Takahashi, A. Triller, and G. Evan. 2004. Differentiation-dependent sensitivity to apoptogenic factors in PC12 cells. *The Journal of biological chemistry* 279:30983-30993.
49. Ulloth, J.E., F.G. Almaguel, A. Padilla, L. Bu, J.W. Liu, and M. De Leon. 2007. Characterization of methyl-beta-cyclodextrin toxicity in NGF-differentiated PC12 cell death. *Neurotoxicology* 28:613-621.
50. Nguyen, H.N., C. Wang, and D.C. Perry. 2002. Depletion of intracellular calcium stores is toxic to SH-SY5Y neuronal cells. *Brain Res* 924:159-166.
51. Hanahan, D., and R.A. Weinberg. 2000. The hallmarks of cancer. *Cell* 100:57-70.
52. Tweddle, D.A., A.J. Malcolm, M. Cole, A.D. Pearson, and J. Lunec. 2001. p53 cellular localization and function in neuroblastoma: evidence for defective G(1) arrest despite WAF1 induction in MYCN-amplified cells. *The American journal of pathology* 158:2067-2077.
53. Park, M.T., and S.J. Lee. 2003. Cell cycle and cancer. *Journal of biochemistry and molecular biology* 36:60-65.
54. Li, W., A. Sanki, R.Z. Karim, J.F. Thompson, C. Soon Lee, L. Zhuang, S.W. McCarthy, and R.A. Scolyer. 2006. The role of cell cycle regulatory proteins in the pathogenesis of melanoma. *Pathology* 38:287-301.
55. Kuiper, R.P., E.F. Schoenmakers, S.V. van Reijmersdal, J.Y. Hehir-Kwa, A.G. van Kessel, F.N. van Leeuwen, and P.M. Hoogerbrugge. 2007. High-resolution genomic profiling of childhood ALL reveals novel recurrent genetic lesions affecting pathways involved in lymphocyte differentiation and cell cycle progression. *Leukemia* 21:1258-1266.
56. Zhu, X., A.K. Raina, and M.A. Smith. 1999. Cell cycle events in neurons. Proliferation or death? *The American journal of pathology* 155:327-329.
57. Jiang, Y., H.I. Saavedra, M.P. Holloway, G. Leone, and R.A. Altura. 2004. Aberrant regulation of survivin by the RB/E2F family of proteins. *The Journal of biological chemistry* 279:40511-40520.
58. Ebelt, H., N. Hufnagel, P. Neuhaus, H. Neuhaus, P. Gajawada, A. Simm, U. Muller-Werdan, K. Werdan, and T. Braun. 2005. Divergent siblings: E2F2 and E2F4 but not E2F1 and E2F3 induce DNA synthesis in cardiomyocytes without activation of apoptosis. *Circulation research* 96:509-517.
59. Parisi, T., T.L. Yuan, A.M. Faust, A.M. Caron, R. Bronson, and J.A. Lees. 2007. Selective requirements for E2f3 in the development and tumorigenicity of Rb-deficient chimeric tissues. *Molecular and cellular biology* 27:2283-2293.
60. Xiong, Y., H. Zhang, and D. Beach. 1993. Subunit rearrangement of the cyclin-dependent kinases is associated with cellular transformation. *Genes & development* 7:1572-1583.
61. Zhou, Q., Z.K. Melkoumian, A. Lucktong, M. Moniwa, J.R. Davie, and J.S. Strobl. 2000. Rapid induction of histone hyperacetylation and cellular differentiation in human breast tumor cell lines following degradation of histone deacetylase-1. *The Journal of biological chemistry* 275:35256-35263.

62. Rieff, H.I., L.T. Raetzman, D.W. Sapp, H.H. Yeh, R.E. Siegel, and G. Corfas. 1999. Neuregulin induces GABA(A) receptor subunit expression and neurite outgrowth in cerebellar granule cells. *J Neurosci* 19:10757-10766.
63. Fallon, K.B., N. Havlioglu, L.H. Hamilton, T.P. Cheng, and S.L. Carroll. 2004. Constitutive activation of the neuregulin-1/erbB signaling pathway promotes the proliferation of a human peripheral neuroepithelioma cell line. *Journal of neuro-oncology* 66:273-284.
64. Herrup, K., R. Neve, S.L. Ackerman, and A. Copani. 2004. Divide and die: cell cycle events as triggers of nerve cell death. *J Neurosci* 24:9232-9239.
65. Potter, S.M. 2001. Distributed processing in cultured neuronal networks. *Progress in brain research* 130:49-62.
66. Ding, X.L., J. Husseman, A. Tomashevski, D. Nochlin, L.W. Jin, and I. Vincent. 2000. The cell cycle Cdc25A tyrosine phosphatase is activated in degenerating postmitotic neurons in Alzheimer's disease. *The American journal of pathology* 157:1983-1990.
67. Becker, E.B., and A. Bonni. 2004. Cell cycle regulation of neuronal apoptosis in development and disease. *Progress in neurobiology* 72:1-25.
68. Carterson, A.J., K. Honer zu Bentrup, C.M. Ott, M.S. Clarke, D.L. Pierson, C.R. Vanderburg, K.L. Buchanan, C.A. Nickerson, and M.J. Schurr. 2005. A549 lung epithelial cells grown as three-dimensional aggregates: alternative tissue culture model for Pseudomonas aeruginosa pathogenesis. *Infection and immunity* 73:1129-1140.
69. Straub, T.M., K. Honer zu Bentrup, P. Orosz-Coghlan, A. Dohnalkova, B.K. Mayer, R.A. Bartholomew, C.O. Valdez, C.J. Bruckner-Lea, C.P. Gerba, M. Abbaszadegan, and C.A. Nickerson. 2007. In vitro cell culture infectivity assay for human noroviruses. *Emerging infectious diseases* 13:396-403.
70. Raguenez, G., L. Desire, V. Lantrua, and Y. Courtois. 1999. BCL-2 is upregulated in human SH-SY5Y neuroblastoma cells differentiated by overexpression of fibroblast growth factor 1. *Biochemical and biophysical research communications* 258:745-751.
71. Wang, C.X., J.H. Song, D.K. Song, V.W. Yong, A. Shuaib, and C. Hao. 2006. Cyclin-dependent kinase-5 prevents neuronal apoptosis through ERK-mediated upregulation of Bcl-2. *Cell death and differentiation* 13:1203-1212.
72. Li, G.N., L.L. Livi, C.M. Gourd, E.S. Deweerd, and D. Hoffman-Kim. 2007. Genomic and morphological changes of neuroblastoma cells in response to three-dimensional matrices. *Tissue engineering* 13:1035-1047.
73. Low, H.P., T.M. Savarese, and W.J. Schwartz. 2001. Neural precursor cells form rudimentary tissue-like structures in a rotating-wall vessel bioreactor. *In vitro cellular & developmental biology* 37:141-147.
74. Pulliam, L., B.G. Herndier, N.M. Tang, and M.S. McGrath. 1991. Human immunodeficiency virus-infected macrophages produce soluble factors that cause histological and neurochemical alterations in cultured human brains. *The Journal of clinical investigation* 87:503-512. 28. Tekautz, T.M., K. Zhu, J. Grenet, D. Kaushal, V.J. Kidd, and J.M. Lahti. 2006. Evaluation of IFN-gamma effects on apoptosis and gene expression in neuroblastoma--preclinical studies. *Biochimica et biophysica acta* 1763:1000-1010.
75. Tekautz, T.M., K. Zhu, J. Grenet, D. Kaushal, V.J. Kidd, and J.M. Lahti. 2006. Evaluation of IFN-gamma effects on apoptosis and gene expression in neuroblastoma--preclinical studies. *Biochimica et biophysica acta* 1763:1000-1010.

76. Kaushal, D., and N. C.W. 2004. Analyzing and Visualizing Expression Data with Spotfire. *Current Protocols in Bioinformatics*

Figure 1. 3-D culture-induced changes in cell division rates and morphology. (A) After 3 wk in RWV culture, the doubling rate of SY cells that were transferred back into 2-D culture for 5 d, drops from 1x/40 h to 1x/65 h, with no change in viability. Data are shown as the mean (n=4) ± SD. * $P<0.001$ (B) SY cells grown in standard 2-D tissue culture flasks, sediment to the bottom surface with a flattened morpology. Culture in a RWV promotes 3-D assembly of the individual cells into large tissue-like aggregates. SEM: scanning electron micrograph.

Figure 2. Decreased expression of N-myc and HuD in 3-D versus 2-D-cultured SY cells. (A) Western blot analysis reveals a progressive decrease in the expression of N-myc and HuD proteins after 2 and 4 wk in 3-D culture that does not occur during growth in 2-D. (B) Confocal images showing expression of the N-myc oncogene and the neuron-specific RNA binding protein HuD. The 3-D culture was maintained for 4 wk. The secondary antibody to N-myc and HuD is labeled with Alexa 488 (green). PI (red) was used as the nuclear stain. The scale bar on each image represents 20 μm.

Figure 3. Resistance to apoptosis is diminished in 3-D cultured SY cells. (A) 1- Confocal microscopy reveals diminished expression of the anti-apoptotic protein Bcl-2 in SY cells cultured for 3 wk in a RWV. Pro-apoptotic Bax and Bak proteins are up-regulated in 3-D culture. The secondary AB to Bcl-2, Bax and Bak is labeled with Alexa 488 (green). PI (red) or To-Pro (blue) was used to stain the nucleus. Scale bars on the images are: Bcl-2 20 μm, Bax 23.81 μm, Bak 40 μm. (A) 2- Western analysis of whole-cell lysates collected from the 3-D and 2-D cultures at 3 wk confirms that Bcl-2 expression is down-regulated in 3-D cells, and expression of Bax is up. (B)1- The percent of TUNEL-positive SY cells in 3-D culture increased 4 to 7 fold

above those in 2-D when treated with TG (10 nM). (B) 2- TUNEL positive PC12 cells in 3-D increased 3 fold above those in 2-D. For (B) 1 and 2: 3-D pre-tx = 3-D cells from RWV just before transfer to dish. 2-D+0 = 2-D cells, unstimulated, 2-D+TG = 2-D cells stimulated with TG, 3-D+0 = 3-D cells, unstimulated, 3-D+TG = 3-D cells removed from RWV to dish, stimulated with TG, 3-D(RWV) +TG = 3-D cells treated with TG inside of the RWV. Data are shown as the mean (n=3) ± SD. *P<0.01 in SY (except for the 3-DRWV+TG where n=1) *P<0.035 in PC12. L axis: actual percent apoptosis R axis: arbitrary units of fold change representing the actual apoptosis.

Figure 4. 3-D culture driven changes in the phenotypic differentiation markers N-myc and Bcl-2 are still apparent after 5 d of return to 2-D growth in tissue culture flasks. After 10 d of re-introduction to 2-D growth, marker expression in the 3-D cultured cells has returned to a level more analogous to those of the 2-D-cultured cell line. The secondary AB to N-myc and Bcl-2 is labeled with Alexa 488 (green). PI (red) was used as the nuclear stain. The scale bars on the 2-D and 3-D images represent 20 μm except for 5 d which represents 40 μm.

Figure 5. Comparison of gene expression in 2-D and 3-Dcultured SY cells using microarray analysis. (A) Changes in gene expression due to cell culture conditions affect cellular disease-related pathways (top three of 63, shown in order of significance). Threshold = cutoff for P< 0.05. (B) Ten canonical pathways most affected in SY cells grown in 3-D rather than 2-D . Bar graph = ratio of gene expression in 3-D cultured cells as compared to those grown in 2-D. Line graph represents significance as –log(p-value) with P<0.05. (C) 1- (Table 1) Gene expression pathway for G1/S cell cycle progression. Values were obtained using IPA software, version 5.0.

Minimum fold change ≥1.5. 2- (Table 2) Confirmation of array results using QRT-PCR. Reactions were run in triplicate with GAPDH gene expression being used as the reference. PCR efficiencies, average fold change and statistical analysis was performed using the REST© software program. All genes in this pathway were represented on the chips. Red: increased gene expression. Green: decreased gene expression. mRNA for the QRT-PCR and array analysis was collected at passage 8 (2-D and 3-D cultures) with n = 2 for each culture type.

Supplemental Data:

Microarray data are annotated both in terms of universal gene symbols (Gene Symbol) and known gene function (Gene Description). Microarray experiments were performed on three biologically replicate Human Exonic Evidence based Oligonucleotide arrays (#s 53383, 53384 and 52791). Differentially expressed genes were selected on the basis of statistical significance using One-way Analysis of Variance (p value) and magnitude of change in gene-expression on a $\log_2$ scale (M). We considered a magnitude change of 50% (1.5 –fold) along with $P < 0.05$ as significant.

C (1)

Table 1

HUGO Gene Symbol	Description	Log Ratio	Location	Type	Entrez Gene ID (H)
CDKN2B	cyclin-dependent kinase inhibitor 2B (INK4, p15, inhibits CDK4)	+3.348	Nucleus	transcription regulator	1030
E2F3	E2F transcription factor 3	-2.15	Nucleus	transcription regulator	1871
HDAC2	histone deacetylase 2	-2.236	Nucleus	transcription regulator	3066
NRG1	neuregulin 1	-4.403	Nucleus	Extracellular Space	3084
RB1	retinoblastoma 1 (including osteocarcinoma)	-1.574	Nucleus	transcription regulator	5925
SKP1A	S-phase kinase-associated protein 1A (p19A)	-1.325	Nucleus	transcription regulator	6500

Molecules associated with cell cycle G1/S checkpoint regulation in SY 2-D and 3-D cells above 50% change.

C (2)
Table 2

Gene	3-D (fold change)	p-value
*CDKN2	+4.04	0.001
E2F3	+1.00	0.947
*HDAC2	-1.57	0.050
*NRG1	-2.39	0.001

Differential expression of selected SY genes in 3-D culture as compared to 2-D. * p≤ 0.05

Figure 1.

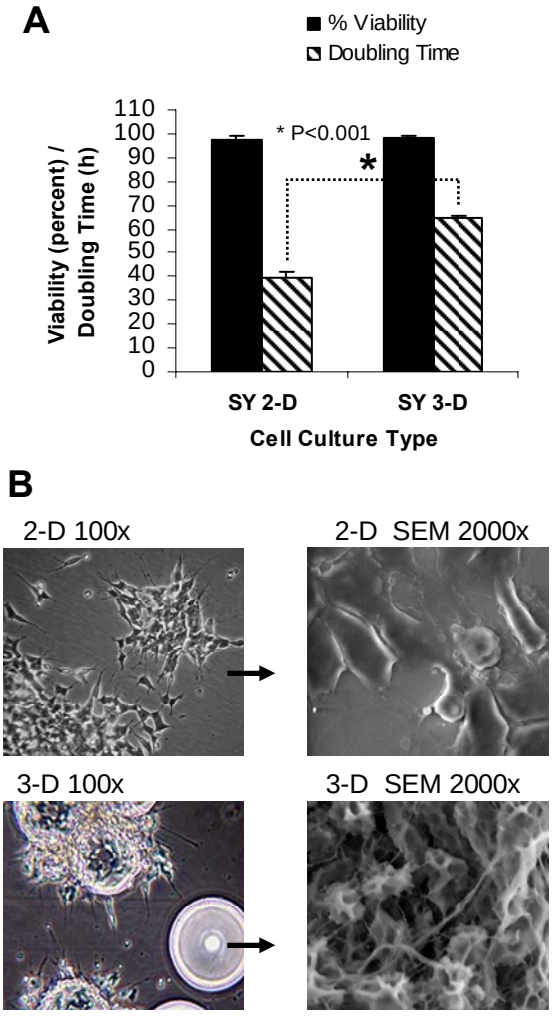
A
% Viability
Doubling Time
Viability (percent) / Doubling Time (h)
110
100
90
80
70
60
50
40
30
20
10
0
* P<0.001
*
SY 2-D
SY 3-D
Cell Culture Type
B
2-D 100x
2-D SEM 2000x
3-D 100x
3-D SEM 2000x

Figure 2.

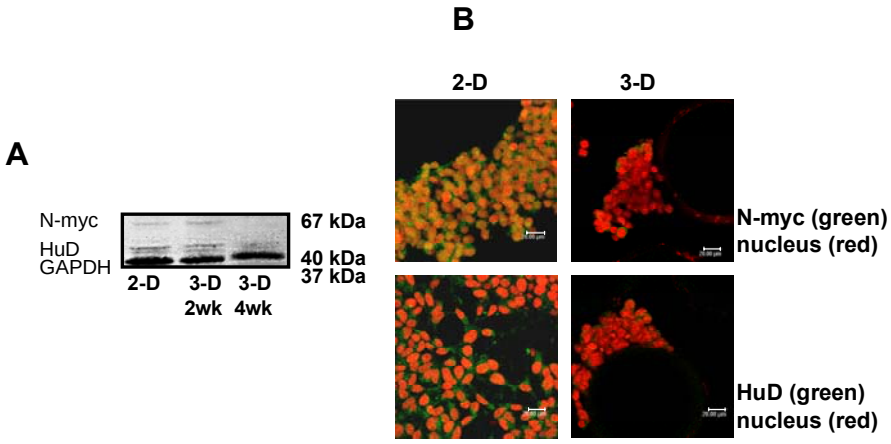
A
N-myc
HuD
GAPDH
67 kDa
40 kDa
37 kDa
2-D
3-D 2wk
3-D 4wk
B
2-D
3-D
N-myc (green)
nucleus (red)
HuD (green)
nucleus (red)

1

Figure 3.

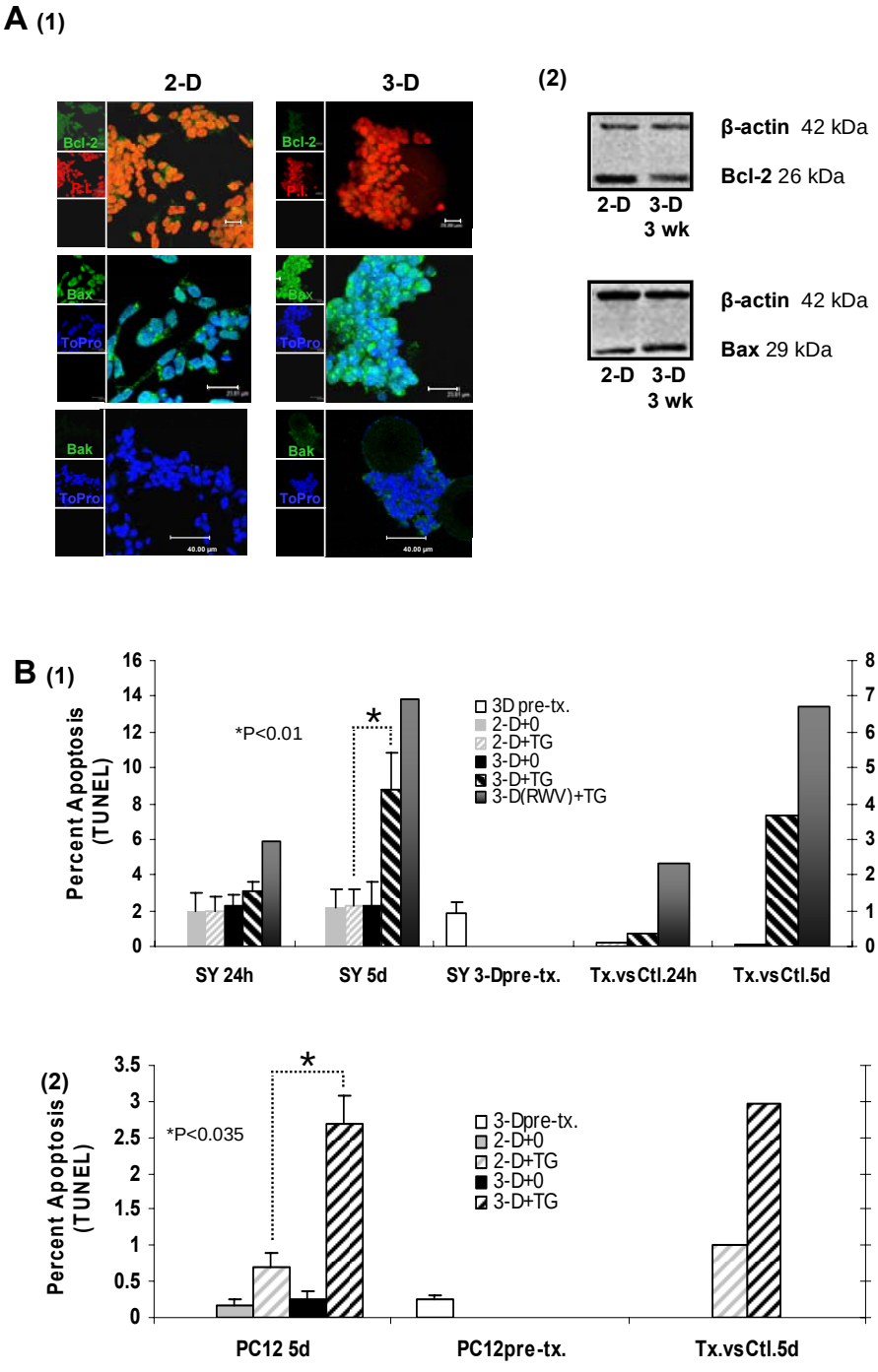
A (1)
2-D
3-D
Bcl-2
PI
Bax
ToPro
Bak
ToPro
(2)
β-actin 42 kDa
Bcl-2 26 kDa
2-D 3-D
3 wk
β-actin 42 kDa
Bax 29 kDa
2-D 3-D
3 wk
B (1)
Percent Apoptosis (TUNEL)
Fold Change
*P<0.01
3D pre-tx.
2-D+0
2-D+TG
3-D+0
3-D+TG
3-D(RWV)+TG
SY 24h
SY 5d
SY 3-Dpre-tx.
Tx.vsCtl.24h
Tx.vsCtl.5d
(2)
Percent Apoptosis (TUNEL)
Fold Change
*P<0.035
3-Dpre-tx.
2-D+0
2-D+TG
3-D+0
3-D+TG
PC12 5d
PC12pre-tx.
Tx.vsCtl.5d

1

Figure 4.

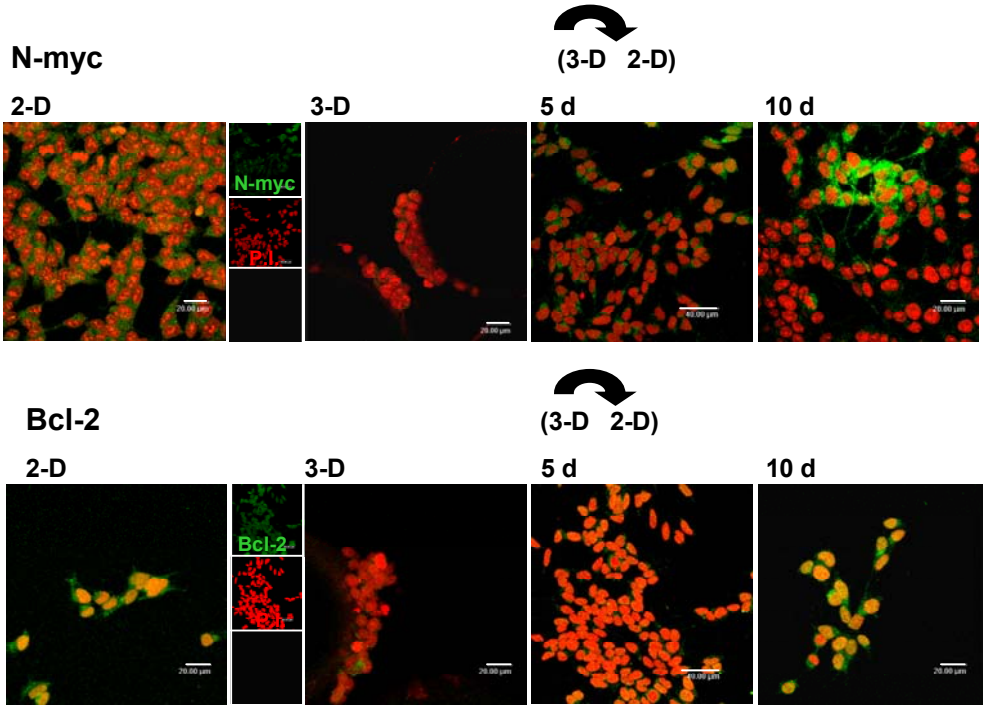

Figure 5.

A

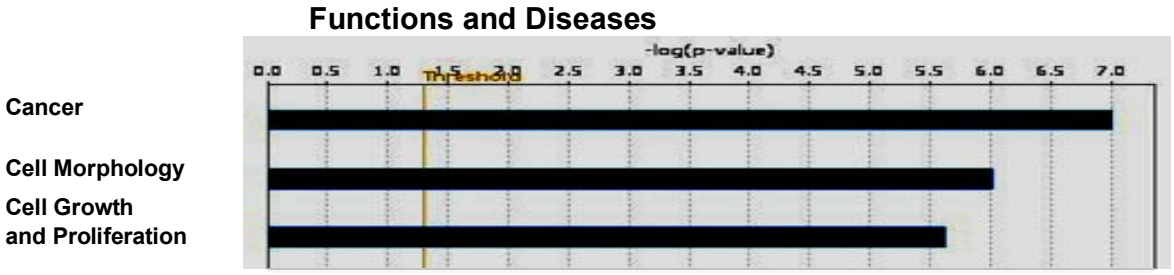
Functions and Diseases
-log(p-value)
0.0 0.5 1.0 1.5 2.0 2.5 3.0 3.5 4.0 4.5 5.0 5.5 6.0 6.5 7.0
Threshold
Cancer
Cell Morphology
Cell Growth and Proliferation

B

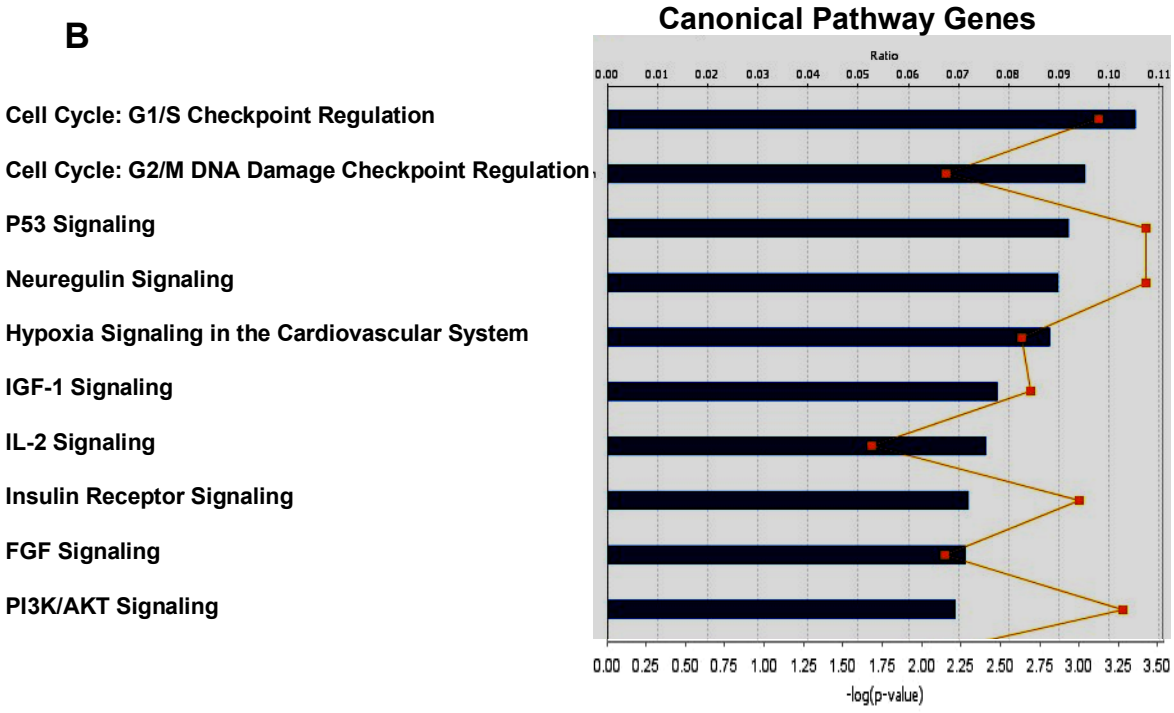
Canonical Pathway Genes
Ratio
0.00 0.01 0.02 0.03 0.04 0.05 0.06 0.07 0.08 0.09 0.10 0.11
Cell Cycle: G1/S Checkpoint Regulation
Cell Cycle: G2/M DNA Damage Checkpoint Regulation
P53 Signaling
Neuregulin Signaling
Hypoxia Signaling in the Cardiovascular System
IGF-1 Signaling
IL-2 Signaling
Insulin Receptor Signaling
FGF Signaling
PI3K/AKT Signaling
0.00 0.25 0.50 0.75 1.00 1.25 1.50 1.75 2.00 2.25 2.50 2.75 3.00 3.25 3.50
-log(p-value)

C (1)

Cell Cycle: G1/S Checkpoint Regulation